AGU PUBLICATIONS

Water Resources Research

RESEARCH ARTICLE
10.1002/2015WR018354

Acoustic mapping velocimetry

M. Muste[1], S. Baranya[2], R. Tsubaki[3], D. Kim[4], H. Ho[5], H. Tsai[1], and D. Law[1]

[1]IIHR-Hydroscience and Engineering, University of Iowa, Iowa City, Iowa, USA, [2]Department of Hydraulic and Water Resources Engineering, Budapest University of Technology and Economics, Budapest, Hungary, [3]Department of Civil Engineering, Nagoya University, Nagoya, Japan, [4]Civil and Environmental Engineering, College of Engineering, Dankook University, Yongin-si, Geyonggi-do, South Korea, [5]Department of Ocean Science and Engineering, Zhejiang University, Hangzhou, China

Key Points:
- Acoustic mapping velocimetry is a novel method to measure riverine bed load transport indirectly
- The method combines optical and acoustic techniques
- A proof-of-concept experiment for AMV is presented

Correspondence to:
S. Baranya,
baranya.sandor@epito.bme.hu

Citation:
Muste, M., S. Baranya, R. Tsubaki, D. Kim, H. Ho, H. Tsai, and D. Law (2016), Acoustic mapping velocimetry, *Water Resour. Res.*, *52*, doi:10.1002/2015WR018354.

Received 9 NOV 2015
Accepted 2 MAY 2016
Accepted article online 5 MAY 2016

Abstract Knowledge of sediment dynamics in rivers is of great importance for various practical purposes. Despite its high relevance in riverine environment processes, the monitoring of sediment rates remains a major and challenging task for both suspended and bed load estimation. While the measurement of suspended load is currently an active area of testing with nonintrusive technologies (optical and acoustic), bed load measurement does not mark a similar progress. This paper describes an innovative combination of measurement techniques and analysis protocols that establishes the proof-of-concept for a promising technique, labeled herein Acoustic Mapping Velocimetry (AMV). The technique estimates bed load rates in rivers developing bed forms using a nonintrusive measurements approach. The raw information for AMV is collected with acoustic multibeam technology that in turn provides maps of the bathymetry over longitudinal swaths. As long as the acoustic maps can be acquired relatively quickly and the repetition rate for the mapping is commensurate with the movement of the bed forms, successive acoustic maps capture the progression of the bed form movement. Two-dimensional velocity maps associated with the bed form migration are obtained by implementing algorithms typically used in particle image velocimetry to acoustic maps converted in gray-level images. Furthermore, use of the obtained acoustic and velocity maps in conjunction with analytical formulations (e.g., Exner equation) enables estimation of multidirectional bed load rates over the whole imaged area. This paper presents a validation study of the AMV technique using a set of laboratory experiments.

1. Introduction

Knowledge of sediment dynamics in rivers is of great importance for several practical applications. Sediment movement in the forms of both bed load and suspended load directly influences aquatic ecosystems, fluvial navigation, hydropower, and water supply. Despite the importance of sediment-related problems in riverine environments, monitoring sediment transport remains a major issue for river engineers and geographers mainly due to the challenges of the measurement process. The estimation of bed load transport rates, which is the main concern in this paper, is made with a diversity of semiempirical equations, which demonstrates that the full understanding of the movement of bed form migration is complex and not fully resolved [*Aberle et al*., 2012]. A necessary step in advancing our predictive formulation in this area is to increase our capabilities to better observe the morphodynamics of the bed form and quantify their relationships with the flow and suspended sediment processes taking place simultaneously in the water column.

In situ estimation of bed load transport can be made with direct or indirect measurements. Direct measurement of the local bed load transport using conventional sampling methods, such as pressure-difference samplers [e.g., *Helley and Smith*, 1971], is expensive both with respect to time and cost because capturing the significant spatial and temporal bed form variability requires a large number of samples. Moreover, the intrusive nature of the grab and sample measurement methods questions the accuracy and representativeness of the measurement as a whole. Difficulties of direct sampling methods are exacerbated when investigating large rivers, especially during high water regimes. Given the limitations of the direct sampling methods, alternative indirect measurement approaches have been increasingly used to monitor bed load transport [*Gray et al*., 2010]. These methods are labeled as surrogates by *Gray et al*. [2010]. The indirect methods have been continuously progressing since the adoption of acoustic sensing technologies for inland rivers in early 1980s [*Muste et al*., 2007].

The Acoustic Mapping Velocimetry (AMV) method discussed in this paper determines the bed load transport rates based on: (a) sounding river beds with single or multisensor acoustic instruments, (b) scanning a two-dimensional area of the bed to produce an acoustic map, (c) repeating map acquisitions at time intervals commensurate with the movement of the bed form, (d) use of image velocimetry concepts applied to the successive acoustic maps to map the velocity distribution associated with the dune movement, and (e) use of the bed form geometry and velocity fields contained in the mapped area in conjunction with analytical relationships to produce the bed load transport rates. AMV can be used to quantify the dynamics of the bed form migration in any type of subcritical flow regime. However, the estimation of the bed load transport rates as presented here is relevant only for lower regime flows when large, irregular dunes are formed by the sediment moving downstream and the dunes are continuously moving downstream. In order to place AMV in historical context, some of the development efforts made in the past are briefly reviewed below. While the efforts have been extensive, only methods that involve one or more of the AMV components are reviewed.

Indirect bed load transport rates can be estimated using information only on the change in bed form geometry [*Abraham and Kuhnle*, 2006] or coupling information on both bed form geometry and migration velocity [*Aberle et al*., 2012]. The increased availability of the acoustic bed form sounding or scanning technologies and well-developed optical methods facilitate characterization of both the geometric and dynamic variables of the bed forms [*Aberle et al*., 2012]. A precursor to the spatial approach of AMV was longitudinal bed form profiling. Repeated sounding along single-survey lines for estimating bed load transport using the dune tracking method was tested by several researchers [e.g., *Simons et al*., 1965; *Engel and Lau*, 1981; *Kostaschuk et al*., 1989; *Dinehart*, 2002]. Furthermore, *Holmes* [2010] used a fixed-boat acoustic Doppler current profiler (ADCP) to acquire longitudinal transects during a 2 day ADCP deployment. The main limitation of this method is that it assumes that the bed load transport is unidirectional, which is rarely the case in natural conditions.

An alternative approach that is capable of revealing multidirectional bed form movement was used by *Abraham and Kuhnle* [2006] and *Abraham et al*. [2011]. Their method utilizes acoustic maps obtained with high-resolution multibeam-echo sounding. Bed load transport rates are obtained by determining the rates of bed scour using time-sequenced bathymetric data. The method was validated in a laboratory flume by comparing the measured rates of bed scour with direct measurements of bed load transport. Their study showed that for dunes traveling at nearly constant speed with nearly constant shape and no suspended load, the estimated bed load transport is consistent with the results of estimations made using bed form amplitude and speed. Subsequently, the method was used for bed load transport estimates in natural rivers [*Abraham et al*., 2010]. Additional studies involving 2-D bathymetry scanning include the laboratory experiments conducted by *Henning et al*. [2010]. They used a cross-correlation technique applied to digital elevation maps built from repeated scanning of a scale model of Oder River to analyze migration rates. This study, however, does not derive bed load transport rates using the measured migration velocities. A complementary effort of this research is the work of *Aberle et al*. [2012] who developed a novel methodology (based on the general form of the Exner equation) to estimate bed load rates.

The most similar investigative approach to the AMV measurement technique reported in this paper is the study conducted by *Duffy* [2006]. In this study, repetitive multibeam surveys were acquired in the field. The measured bathymetric data set was used to determine bed form migration rates, morphometric parameters, and eventually to calculate net sediment transport. The main differences between our and *Duffy*'s studies are in the cross-correlation technique used to obtain the bed form migration velocity from consecutive digital terrain maps, and in the procedures for validating the bed load transport method. The latter was a difficult task for *Duffy*'s study because of the complexity of the environment used for proving their measurement concept.

This paper focuses on a new bed form tracking technique that combines components and processing protocols from two contemporary nonintrusive approaches: acoustic and image-based. The bed form mapping is conducted with acoustic surveys while the estimation of the velocity of the bed forms is obtained with processing techniques pertaining to image-based velocimetry. Given the combination, we call the technique acoustic mapping velocimetry (AMV). The implementation of this technique produces a whole-field velocity map associated with the multidirectional bed form movement. The paper demonstrates that the nonintrusive AMV technique is capable of: (a) tracking the dynamics of the bed forms in two-dimensional

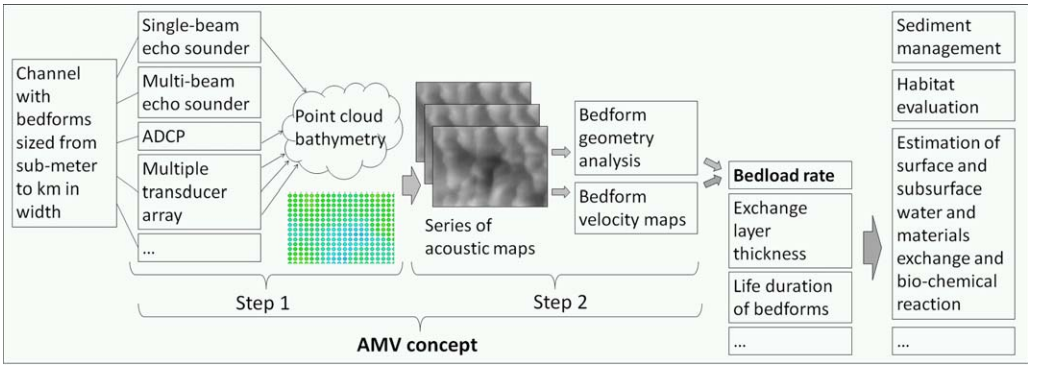

Figure 1. Schematic of the concept of AMV.

space, and (b) providing rates of bed load motion in multiple directions. While the results presented here are obtained in a laboratory environment, the technique can be applied to field conditions, taking advantage of the plethora of acoustic mapping technology available today.

2. AMV Methodology

The implementation of the AMV concept illustrated in Figure 1 entails two processing phases [*Muste et al*., 2015]. In the first step, the acoustic maps are created as a continuous depth-data layer covering the target area of the channel bottom. This step is the basis for all sounding techniques and produces the conventional bathymetric maps. The conventional as well as the acoustic maps are a full 3-D description of the geometry of the bed forms. In the second step, the acoustic maps are converted to an "image-equivalent" through resampling of the raw information. The obtained images are subsequently processed using a version of the image velocimetry technique [*Muste et al*., 2008]. Bed load rates are obtained by combining the outcomes from both acoustic mapping acquired in step 1 and the velocity fields obtained in step 2 with analytical relationships for predicting sediment transport rates for the bed load [*Vanoni*, 2006]. Overviews of the background of steps 1 and 2 are provided below.

2.1. Creation of Bed Form Acoustic Maps

Acoustic maps are 3-D representations of the bed geometry. The maps can be created using different instruments depending on the measurement situation. For field studies, single beam and multibeam echo sounders (MBES) or ADCP can be used for acquiring the maps [*Spasojevic and Muste*, 2002]. Single beam echo sounders and the ADCP provide depth information along lines (tracks), whereas MBES surveys in swaths (i.e., spatial bins aligned in the streamwise direction) that can be easily converted to surfaces of bed elevation with significantly higher resolution than with ADCPs. For laboratory experiments, detection of bed changes can be carried out with ultrasonic bed profilers equipped with a single sensor or multiple sensors arranged as linear or areal arrays. Similarly to MBES, the array of sensors is more proficient as it scans with multiple points [*Ho et al*., 2012]. Regardless of the instrument used and measurement situation, the acoustic sensors output is a cloud-like data set of bed-elevation points replicating the shape of the bottom of the water body during the survey. If sampled with sufficient density, the discrete depth values acquired by each sensor can be interpolated to obtain a map of the channel bottom.

Irrespective of the experimental situation (i.e., laboratory or field conditions), there are important considerations that need attention prior to mapping with acoustic survey instruments. Similarly to the recording of a photographic snapshot (whereby all the image pixels are captured at the same instant), the acoustic map should ideally contain depth measurements acquired simultaneously over the whole mapped area. This is however difficult to attain using instruments that construct the map by scanning the target area with individual sensors or (at best) with sensors arranged as linear arrays of finite extent. Given that the depth measurements are not acquired simultaneously, the obtained map will be unavoidably affected by the movement of the bed form during the acquisition of the depth measurements. For a better understanding

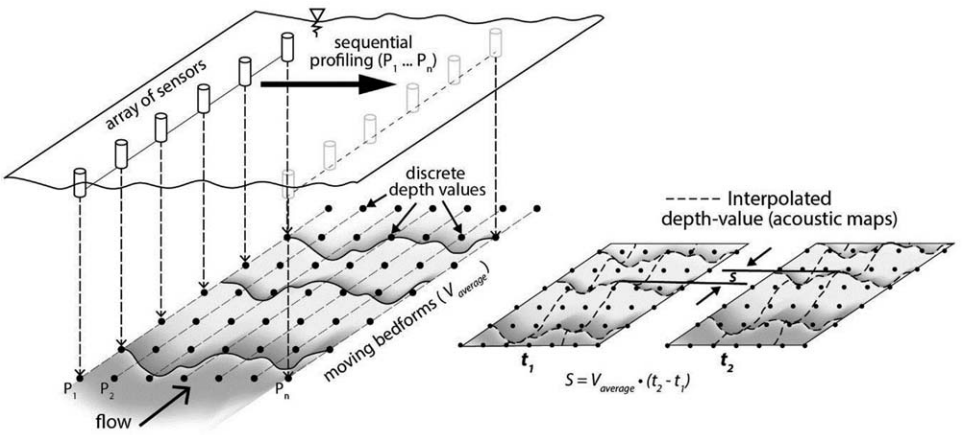

Figure 2. Schematic of the process leading to the creation of acoustic maps using a linear array of acoustic sensors.

of these implications, a linear array of acoustic sensors as used in the present experiments is discussed below (see Figure 2).

Mapping with a linear arrangement of sensors leads to a longitudinal profile of the bed form as shown in Figure 2. The mapping is initiated on one side of the area to be surveyed and continues through successive lateral displacement across the area to be mapped. To attain a prescribed accuracy for longitudinal bed form profiles at each location, it is necessary to average over a number of repeated readings for a single instrument positioning. The number of repetitions is related to the accuracy and sampling frequency of the depth instrument used in the survey. In laboratory conditions for example, the sampling duration at one location is of the order of 1–2 s for a medium quality acoustic sensor. The sensor array is successively positioned over the area targeted for mapping using the same sampling protocol for each measurement location. Closer spacing between the sensors along the linear array and between successive deployment locations yields better resolution in sampling the fine structure of the bed forms.

The duration of the fixed measurements at each location along with the time needed to move the sensor array over the entire area targeted by mapping amounts to a certain time interval that represents the total duration of the mapping. Given that during one mapping the bed forms continue to migrate, the resultant map will unavoidably combine a series of longitudinal bed form profiles taken at slightly different times. This process is akin to other scanning systems used in remote sensing that assume that the time to conduct the scanning is negligible with respect with the velocity of the features in the mapped area. Given the limited capabilities of the instrument data acquisition procedure to acquire all the information in one "shot," there are trade-offs that the operator has to make in order to attain good accuracy and realistic mapping. The main choice that an experimenter has is to shorten the time required for mapping or to reduce the area to be mapped to a size that is manageable for the available instrument and measurement protocol.

In summary, accurate construction of the maps requires development of a measurement protocol that takes into account the characteristics of the instruments, the size of the target map, the time needed to relocate the sensor(s) over the measured area, and geometry and dynamics of the bed forms to be mapped. As intriguing as it sounds, the last consideration needs to be known even before conducting the mapping. From this perspective, before acquiring acoustic maps in a new situation, preliminary measurements should be acquired to roughly assess characteristics of the bed forms (e.g., dune wavelength and other geometrical characteristics) and their dynamics. Based on these preliminary measurements, the spatial coverage of the measurement and the associated protocols can be accordingly adjusted through iterative tests. Once acquired, the acoustic maps are typically presented as color-coded or isocontour maps.

2.2. Estimation of the Bed Form Velocity Maps

While the idea of determining bed load transport using information on bed form geometry and migration speed is widely applied, observing bed form dynamics via processing acoustic maps is novel, and it was inspired by image velocimetry concepts [*Duffy*, 2006]. Essentially, image velocimetry determines probable

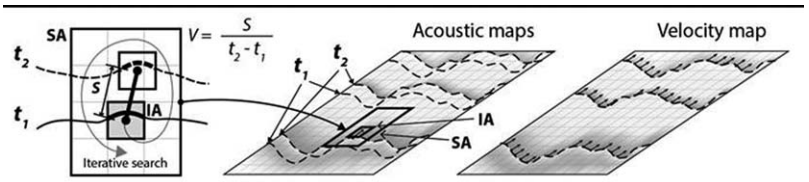

Figure 3. Schematic of the image velocimetry process: (a) selection of the search and interrogation areas; (b) implementation of the pattern matching over the image containing identifiable patterns; and (c) results of the image velocimetry applied over the whole image.

displacements of recognizable patterns embedded in a sequence of images. The displacements are determined using a statistical approach whereby a pattern matching technique is applied to image intensity distribution in a series of images [*Adrian*, 1991; *Fujita et al*., 1998]. The analysis is made successively over the entire imaged area using small interrogation areas (IA) covering the area subjected to measurement, as illustrated in Figure 3a. The similarity index for patterns enclosed in a small IA in an image is calculated for the same-size window within a larger Search Area (SA) selected in the subsequent image. The selection of IA and SA is guided by heuristic rules of thumb [e.g., *Adrian*, 1991; *Raffel et al*., 1998] but typically they are optimized by trial and error for every new application.

The similarity index used for image processing in this paper is estimated using a spatial cross-correlation algorithm [*Fujita et al*., 1998] applied to a pair of acoustic maps (shown in Figure 3b). Fujita's algorithm is based on a cross-correlation approach created by *Fincham and Spedding* [1997] whereby cross-correlation is applied to gray-level patterns in the image rather than point clusters [*Muste et al*., 2008]. The Fincham and Spedding algorithm is similar to the cross-correlation algorithm applied to linear seafloor features embedded in the acoustic maps developed by *Duffy* [2006]. The result of image velocimetry processing is a distributed velocity field uniformly covering the acoustically mapped area (see Figure 3c).

Prior to applying image velocimetry to acoustic maps, the conversion of the acoustic maps to gray-level maps is needed. For this purpose, the depth measurements obtained as described above and color-mapped using red, green, and blue are converted into gray-colored pixels using a scale from 0 to 255. The interpolated color maps are converted in pixel coordinates by successively sampling the entire image. The resolution of the pixel image is decided by the user, but it should be commensurate with the spatial resolution of the mapping and the scale of the bed form spatial features. The technique as described herein is well suited for both field and laboratory conditions. For the validation experiments described in this paper, we used a series of laboratory measurements acquired in a moving-bed open-channel flow experiment to illustrate the feasibility of the AMV concept.

2.3. Determination of Bed Form Geometry

The definition of characteristic bed form geometry is not straightforward as these bed features are generally not regular even under steady flow conditions [*Nordin*, 1971]. In order to describe the spatially complex nature of the bed forms for the bed load estimation, we distinguish the geometric parameters along the cross section. For this purpose, the characteristic bed form heights are estimated for separate longitudinal profiles along the centerline of the strips used for bed load estimation, as detailed in section 4. The characteristic bed form height for each strip is calculated as the mean of individual dunes found along the given line. The height of individual dunes (H_i) along a longitudinal section is defined as the average of two distances (see Figure 4): (i) distance from trough to crest, (ii) distance from crest to trough. There are several methods to find the location of the crests and troughs. For instance, an automatized technique to find these locations and calculate bed form heights was presented by *van der Mark et al*. [2008], who developed a bed form tracking tool. In

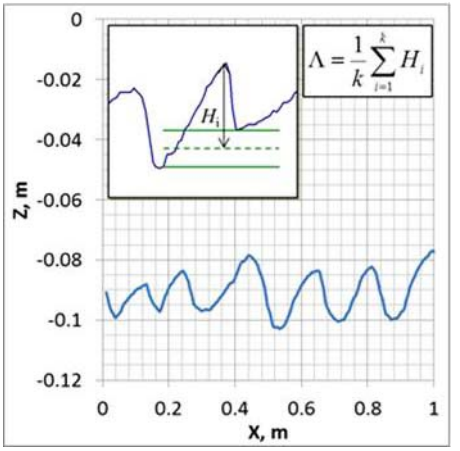

Figure 4. Calculation of bed form height (Λ).

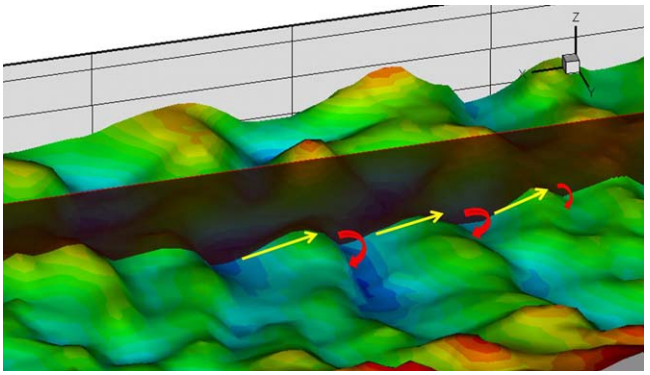

Figure 5. Illustration of the bed form dynamics at the level of bed forms: yellow vectors pertain to the stoss side of dunes, red vectors pertain to the lee side of the bed forms.

this study, however, due to the relatively low number of the bed forms, we manually selected the location of the crests and troughs.

2.4. Quantification of the Bed Load Rates

The whole-field velocity distributions associated with the bed forms within the acoustic maps can be used in conjunction with analytical methods for evaluating bed load rate estimates. This idea is not new and has advanced significantly with the development of new nonintrusive sensors [*Aberle et al*., 2012]. The method selected for this study is based on the continuity equation applied to bed form movement [*Exner*, 1925]:

$$(1-p)\frac{\partial y}{\partial t}+\frac{\partial q_b}{\partial x}=0 \tag{1}$$

where p is the porosity of the river bed, y is the bed elevation, t is the time, q_b is the volumetric bed load transport rate per unit width, and x is the longitudinal distance. Assuming a steady uniform flow and that the dunes are in equilibrium in the domain (including multiple dunes), *Simons et al*. [1965] introduced the following formula for the volumetric bed load per unit width from the macroscopic viewpoint:

$$q_b=(1-p)V_D\frac{\Lambda}{2} \tag{2}$$

where V_D is the bed form velocity and Λ is the bed form height. Averaging over a bed form wavelength shows that the mass transfer of sediment corresponds to the product of the bed form migration velocity and the average thickness of the sediment layer above a base elevation of zero movement [*Aberle et al*., 2012].

Although the equation assumes 1-D bed form movement, in natural situations, there is always a transversal component of the sediment transport which actually does not contribute to the bed load discharge in the downstream direction. However, in this application, we only consider the streamwise component of the bed form velocity in equation (2). The mapped area is split into longitudinal strips that can be obtained in field from MBES swaths [*Abraham et al*., 2010]. The mass of the bed load material transported by the stream can then be estimated by multiplying q_b by the density of the sediment. For practical applications, the most often needed quantity is the cross-sectional bed load transport, that is obtained by integrating q_b along a transect.

In general, equation (2) is applied at the macroscopic level (i.e., 2-D steadily propagating bed forms of unchanging shapes) over the entire channel covering multiple dune lengths. In this study, we utilize the same concept but for smaller spatial scales (i.e., of the order of one dune length or less), therefore we categorize this approach as mesoscopic. The microscopic measurement approach describes the motion of each sediment particle and ripples within one dune length. The mesoscopic approach is employed with the understanding that the bed load migration is nonhomogeneous in space and thus the process is better captured using smaller scales, which leads to improved accuracy in the bed load transport rate estimation compared to the macroscopic approach.

The quantification of the bed load transport rate as presented here assumes that the bed load transport is associated with the downstream movement of the particles. This simplification stems from the fact that while the image patterns travelling on the stoss part of the dunes can be reliably tracked by image velocimetry (yellow vectors in Figure 5), the patterns on the lee face are more difficult to be identified as they are smaller and driven by energetic 3-D velocities (red vectors in Figure 5). Consequently, the total sediment

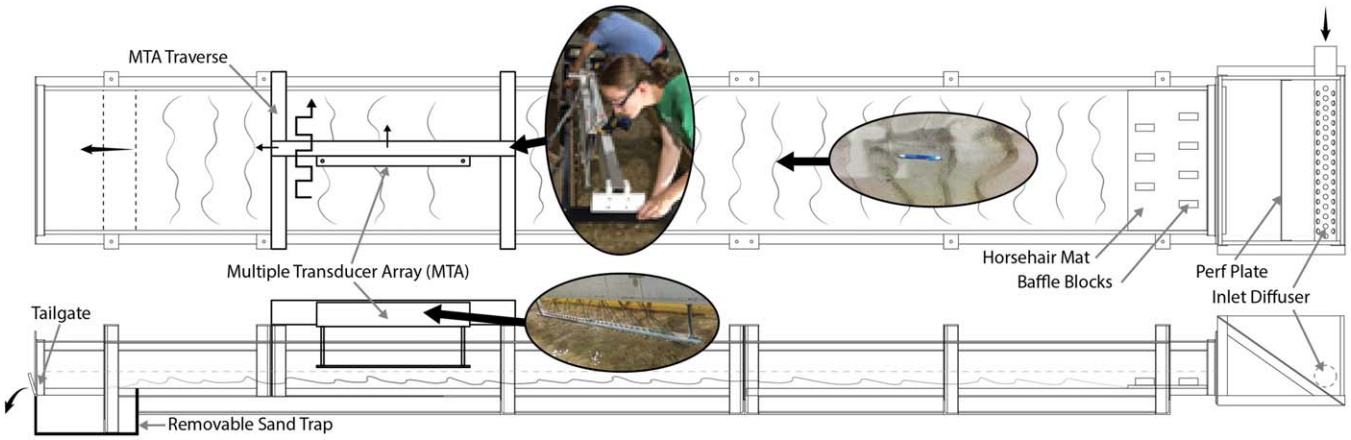

Figure 6. Schematic of the experimental flume, MTA arrangement, and measurement protocols.

flux is positive due to the dominance of the overall downward movement of the particles (as a group or individual). The uncertainty associated with this assumption has not been estimated but can be best tackled using the microscopic approach based on optical techniques [e.g., *Chichibu et al.* 2008] for measuring fluid and sediment velocity fields simultaneously). Additional uncertainties are introduced by the influence of bed form shape, an often-discussed topic in this area [e.g., *Duffy*, 2006] and the porosity or density of the bed sediment.

The estimation of bed load rates using equation (2) entails the following steps:

1. Acquisition of a sequence of acoustic maps (preferably at equal time steps commensurate with the average velocity of the bed forms front).
2. Quantification of bed form dynamics (i.e., calculation of 2-D bed load velocity fields within the mapped area).
3. Determination of the average bed form migration velocities over streamwise strips sized to consider the bed form cross-sectional variability.
4. Determination of characteristic bed form height along the strips enclosed within the mapped area.
5. Estimation of bed load transport per unit width using equation (2) in conjunction with information obtained in steps 3 and 4 for each transect.
6. Integration of specific bed load transport rates over the study cross section.

3. Experimental Arrangements and Protocols

3.1. Facility and Instrumentation

A 6 m long, 0.762 m wide, and 0.40 m deep adjustable slope channel located at IIHR-Hydroscience & Engineering (IIHR) was used for conducting the experiments (see Figure 6). Structural steel frame members provided ample support along the model test section to avoid deflections in the roadway and curb surfaces. The channel was fed with water through a multihole diffuser set in the channel head box. Inflows to the model were measured with a calibrated orifice meter with stated accuracies of $\pm 3\%$ of reading. The flow meter was installed to ASME standards [*ASME*, 1989]. Provisions were made at the channel entrance to condition the flow and increase its turbulence intensity. For this purpose, a series of bluff blocks were set on a thick perforated mat as shown in the figure. Water level was controlled by an adjustable gate set at the channel end. Flow uniformity during the tests was checked using a point gage. Depth readings were acquired at five locations along the channel with periodic repetition to ensure that the flow uniformity is maintained. During the experiments, the slope was adjusted using a set of removable vertical support legs and a pillow block bearing at the downstream end of the channel. During the experiments, the channel slope was set at 0.3%, while discharge varied in the 0.018–0.023 m^3/s range. The hydraulic specifications for the three experimental runs performed in this study are provided in Table 1.

Table 1. Flow Specifications for the Proof-of-Concept Experimental Runs

	Discharge Q (m^3/s)	Flume Width B (m)	Flow Depth H (m)	Mean Velocity U (m/s)	Froude Number (Fr)	Reynolds Number (Re)	Slope (%)	Bed Shear Stress (N/m^2)	u_* (m/s)	d_{50} (mm)	w_s (m/s)	Z_R
RUN 1	0.0227	0.762	0.1	0.3	0.303	30000	0.3	2.94	0.054	0.6	0.093	4.2
RUN 2	0.0198	0.762	0.095	0.27	0.280	25650	0.3	2.80	0.053	0.6	0.093	4.3
RUN 3	0.0181	0.762	0.09	0.26	0.277	23400	0.3	2.65	0.051	0.6	0.093	4.4

Well-sorted coarse sand with $d_{50} = 0.6$mm and $d_{mean} = 0.77$mm was used as bed material. This sand type was successfully used for several previous modeling studies on bed load transport [e.g., *Muste and Ettema*, 2000; *Ho et al*., 2013]. A sand layer, 0.05 m thick, was set on the channel bottom throughout its length. The sand bed was leveled at the beginning of each new experimental run. At the downstream end of the channel, a sediment trap was placed. The final sediment trap volume and interior shape was established using a trial and error approach. The tests were aimed at trapping all the sediment coming out from the channel to accurately quantify the sediment transport in the facility. The tests were conducted over long time intervals and over the whole range of discharges used on the experiments. Following each experimental run, the trapped sand was collected, oven-dried and weighed for estimating transport rates for the bed load.

As shown in Table 1, the bulk bed shear stress values calculated from the mean flow depth and flume slope varied between 2.5 and 3 N/m^2. Using the bed shear velocity (u_*) calculated from bed shear stress and the settling velocity for the d_{50} of the bed material (w_s), calculated by the formula suggested by *Cheng* [2009], the Rouse number (Z_R) is obtained from:

$$Z_R = \frac{w_s}{\kappa u_*} \tag{3}$$

Values of Rouse number in the 4.2–4.4 range suggest that the dominant sediment transport mode is bed load [*Rouse*, 1939] and therefore the suspended sediment transport is neglected.

The bathymetric measurements reported in this paper were acquired in a laboratory setting using a SeaTek Multiple Transducer Array (MTA). MTAs are suitable for bathymetric surveys both in field and laboratory environments (http://seatek.com). The MTA sensors measure depth using high-frequency sound pulses. The travel time principle is at the basis of MTA operation. Specifically, sound wave pulses are transmitted toward the bed where the waves are partially reflected back to the sensor. The sensor records the time for the sound waves to travel from the sensor to the object and back to the sensor. Using the speed of sound in the medium and the recorded travel time of the pulse, the distance from the sensor to the reflective object is estimated, which is then converted into bed elevation reported in the instrument's coordinate system. The relevant characteristics of the individual MTA sensors used in the present study are summarized in Table 2.

For the experimental conditions in the present study ($\sim$ 0.10 m depth), the instrument footprint diameter is 0.005 m. The accuracy of the acoustic sensor is variable depending on multiple factors as illustrated by *Hanes et al*. [2001]. The study finds for their measurement conditions that the accuracy ranges from 0.15 to 0.3 mm.

This instrument has been successfully used for bathymetric measurements in previous laboratory shallow flows by *Friedrich et al*. [2005], *Abraham and Kuhnle* [2006], and *Lin* [2011]. The sensor array manufacturer provides a DOS-based data acquisition package, which outputs an ASCII file containing raw bathymetry measurement and time stamps. However, no MTA-associated post processing software is currently available for processing the dynamics of the measured bathymetric profiles. A customized plug-in software for the MTA was developed for this study to ingest the depth measurements in a customized processing database.

Table 2. MTA Specifications (www.seatek.com)

SeaTek MTA System	
Operating frequency	5 MHz
Transducer diameter	0.0125 m
Depth range	0.03–1.10 m
Max scan rate	0.2 s

3.2. Experimental Protocols

The variables measured for controlling the flow conditions during the experiments included water depth at several locations, incoming

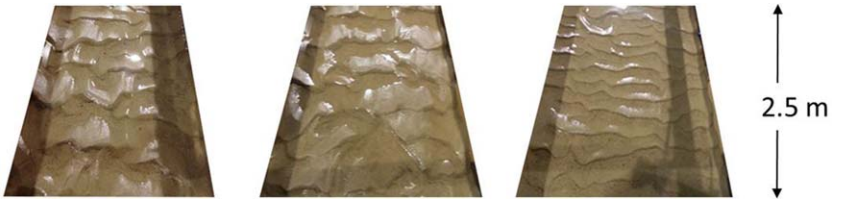

Figure 7. Photos of the bed forms obtained in Runs 1, 2, and 3. Flow from top to bottom.

discharge, volumes and weight of trapped sand, and temperature. In addition to the above, measurements with the MTA were acquired using a protocol separately described below. Prior to each production test, an extensive number of runs were conducted to ensure flow and bed form uniformity and to determine the duration over which these conditions are maintained in the test section. Given that the purpose of the production test was to compare two alternative measurement techniques, rather than accurate replication of a bed load transport processes, the sediment was supplied by the eroded material in the upstream section of the channel. Before each production run, the flume was set up and run for an extended period of time (about one day) to reach equilibrium and create even distribution of the bed forms. The experiments were conducted the day after setting the equilibrium flow with a special protocol that replicated the flow leading to the bed form creation without disturbing the existing bed forms. During these tests, it was found that the facility could sustain uniform transport rates for up to 8 h by continuous erosion of the material in the upstream scour hole without visible nonuniform depositions along the flume. The volumes of bed scour, sand deposit immediately downstream the scoured area, and trapped material were all estimated to verify that the flow was in equilibrium for each run and replicable for the same hydraulic conditions. Visual inspection and point gage measurements of the bed in the test section were made to verify that the test section was in equilibrium throughout the experiment. A view of the bed in the test section during the three production tests is provided in Figure 7.

The mapping was performed with a MTA containing 32 sensors spaced at 3.17 cm apart. The array of sensors, illustrated in Figure 6, was set on a traverse to allow precision control of its position in the streamwise and spanwise directions. Motion of the MTA parallel to the flow was controlled with two clamps placed along the support beam upon which the MTA rested (one flush against one side of the MTA, and the other 1.59 cm from the opposite side). Motion perpendicular to the flow was quantified and controlled visually by two measuring tapes attached to the cross bars that the support beam rested on, as illustrated in Figure 6. Mapping of the bed forms started with the MTA positioned on the same side of the flume for each trial (see Figure 6 and 8). Once the MTA had finished sampling at the first position (up to 2 seconds), it was moved to the next position, 1.5 cm in the downstream direction, and the bed form heights were sampled again. From this position, the array was slid to a new position 1.5 cm away in the transverse direction. Thus a ladder

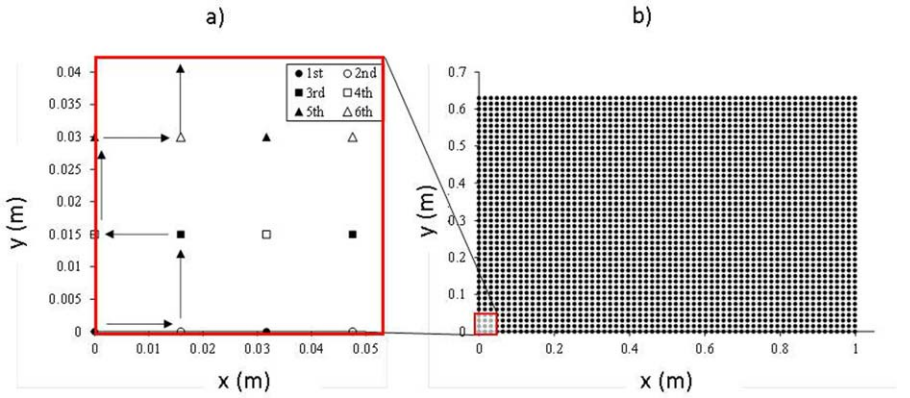

Figure 8. Creation of the acoustic maps: (a) stepwise arrangement for collection of the depth measurements (the arrows on the left side of the figure trace the progression of one MTA sensor during the mapping); (b) the depth measurement points for one mapping of the test area.

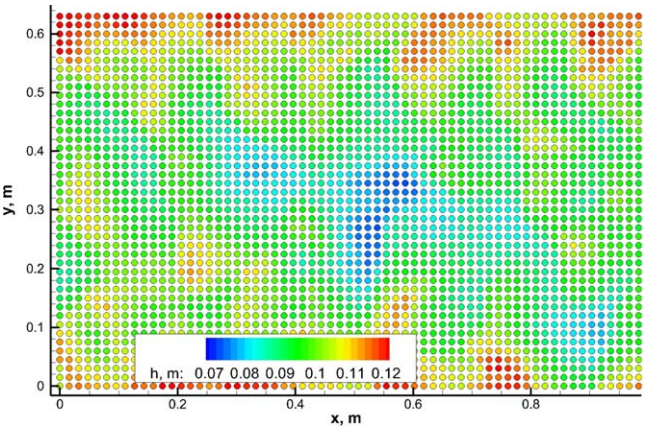

Figure 9. Example of an acoustic map created from the MTA scanning (run 1, first map).

pattern was established as the MTA moved across the flume as shown below, which yielded a resolution of roughly 1.6 cm × 1.6 cm.

Each bed elevation point was sampled for 1 to 2 s at 5 Hz. The sampling time was established through preliminary tests to account for the probe accuracy and noise level in individual measurements. The side-to-side travel time for the MTA took 10 min to complete. The bed form movement during the 10 min travel inherently induced a continuous distortion in the mapped bed form from the position and shape at the time of the initiation of the mapping. The largest distortion, occurring between the starting and ending sides of each map, was assessed with video recordings at about 1.5 cm. Given this inherent measurement method limitation, it was critical to keep the mapping time strictly constant for all the acquired maps such that the distortion of each map would be similar. A 10 min break was taken following each map, followed by another mapping. No less than five consecutive maps were acquired for a given target flow rate.

4. Bedload Estimation Using AMV

4.1. Building of Acoustic Maps

Three sets of experiments were carried out at three different flow discharges. The flow depth at the outlet section was kept constant for each run with an average value of 0.1 m. The flow discharges for Runs 1, 2, and 3 were 0.0227, 0.0198, and 0.0181 m^3/s, respectively. The measurements were performed at uniform flow conditions which were checked with water surface profiling and visual observations. During preliminary tests, it was be observed that it took about one day of continuous flow over the sand-bed flume to bring the original flatbed to dynamic equilibrium conditions with fully developed bed forms. The bed form mapping started the next day after attaining the equilibrium, using carefully controlled protocols. The equilibrium was verified by periodically checking the amount of bed material that was retained in the sand trap. Another indicator of the status of the bed forms was visual observation of the bed, which at equilibrium presented well-defined bed forms with similar characteristics all along the test area. Five acoustic maps were subsequently acquired for each production run. The maps were acquired in the flume test section and are 1.0 long and 0.64 m wide, as illustrated in Figure 9.

4.2. Converting Maps to Images

The image processing software is applied to raster images, therefore the scatter points provided by the multiarray bed scanning method had to be converted into images. The transformation entails two steps. In the first step, the scatter points are triangulated to get a continuous surface of the flume bed. For this purpose, a linear interpolation is applied to obtain depth information between points with measured depth values. The depths were converted to gray-level contour images, as illustrated in Figure 10. Light gray zones indicate deep bed areas (low elevations) while dark patches indicate shallower flow areas (higher bed elevations). In the second step, the optimal resolution of the acoustic images is determined considering two desired outcomes: (i) attaining a reasonably fine resolution that is accurately replicating the bed form geometry, and (ii) limiting the output image size, as the computational demand of processing the images increases with the pixel number. After several preliminary tests, the optimum pixel size was found to be 0.003 m. This pixel resolution was uniformly applied to all acoustic mapping conversions.

Five acoustic maps were generated for each experiment. The time intervals between the maps were about 20 min. For illustration purposes, four gray-level acoustic maps from the first experiment are provided in Figure 10. The maps allow for observation of the 3-D bed forms developed along the flume with a characteristic wavelength of ∼0.20 m and a trough-to-crest height of ∼0.02 m. The obtained images are

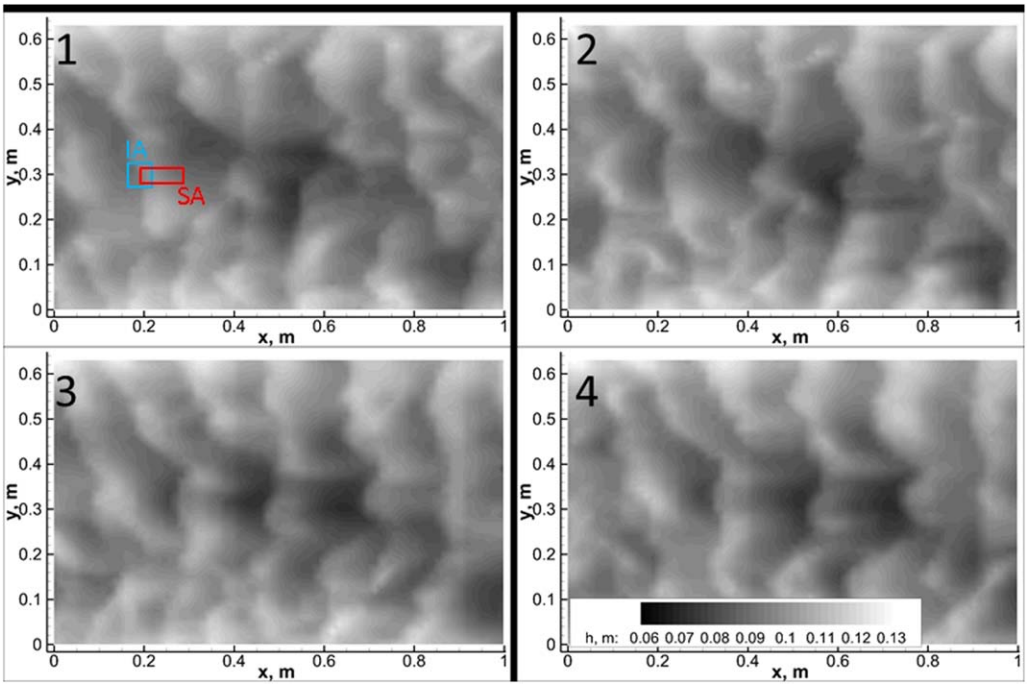

Figure 10. A sequence of gray-level acoustic images for Run 1.

characterized by adequate spatial resolution as the characteristic parts of the bed forms, such as the stoss face, the crest, lee face, and trough, can be clearly distinguished. The images show that a narrow area along the flume walls displays overall deeper flows compared to the central area where the opposite can be observed. The difference is attributed to the flume artifacts. Specifically, the presence of the wall induces additional stresses that enhance the sediment transport locally. This artifact does not affect the results of the experiments, as the goal of the validation experiment presented herein is to capture the cross-sectional bed load transport, similarly with what is targeted in field conditions.

4.3. Quantification of the Bed Form Morphodynamics

Using the maps generated above, an image velocimetry procedure was applied to quantify the displacement of identifiable bed form features within pairs of acoustic maps recorded at successive times. The image processing software applied for processing is called Large Scale Particle Image Velocimetry (LSPIV). LSPIV has extensively been used for estimation of free-surface velocity distributions in rivers [e.g., *Muste et al.*, 2008; *Kantoush et al.*, 2011]. The optimum sizes for the interrogation area (IA) and search area (SA) were determined based on a trial-and-error tests conducted before processing the acoustic maps obtained from the experimental runs. Use of large areas for these parameters smoothen out the spatially heterogeneous information while the use of small values for the parameters result in poor cross-correlation coefficients that are quality indicators for the image processing algorithm and used in the software as a filtering criterion. The preliminary tests indicated that an interrogation area of 0.06 $\times$ 0.06 m and a search area of 0.03 $\times$ 0.09 m were optimal for the current situation. Frame 1 in Figure 10 displays the actual sizes of the SA and IA superposed onto the bed image.

Application of the image velocimetry procedure quantifies the bed form migration with associated velocity maps. Sample results of LSPIV processing applied to acoustic maps are shown in Figure 11 where the velocity distributions superposed on the color-coded map of velocity intensity (as isocontours) are shown using the first pairs of images from Run 1, Run 2, and Run 3, respectively. The plots in the figure display velocity vectors using a spatial resolution of 0.01 m. Zones without velocity vectors are areas where the correlation coefficient is poor hence the results are discarded. If the density of the vectors in the surrounding area is suitable, interpolation schemes can be used to fill in the missing vectors. The range of the velocities in the experiments is between $5{\cdot}10^{-6}-6{\cdot}10^{-5}$ m/s or 0.018–0.216 m/h.

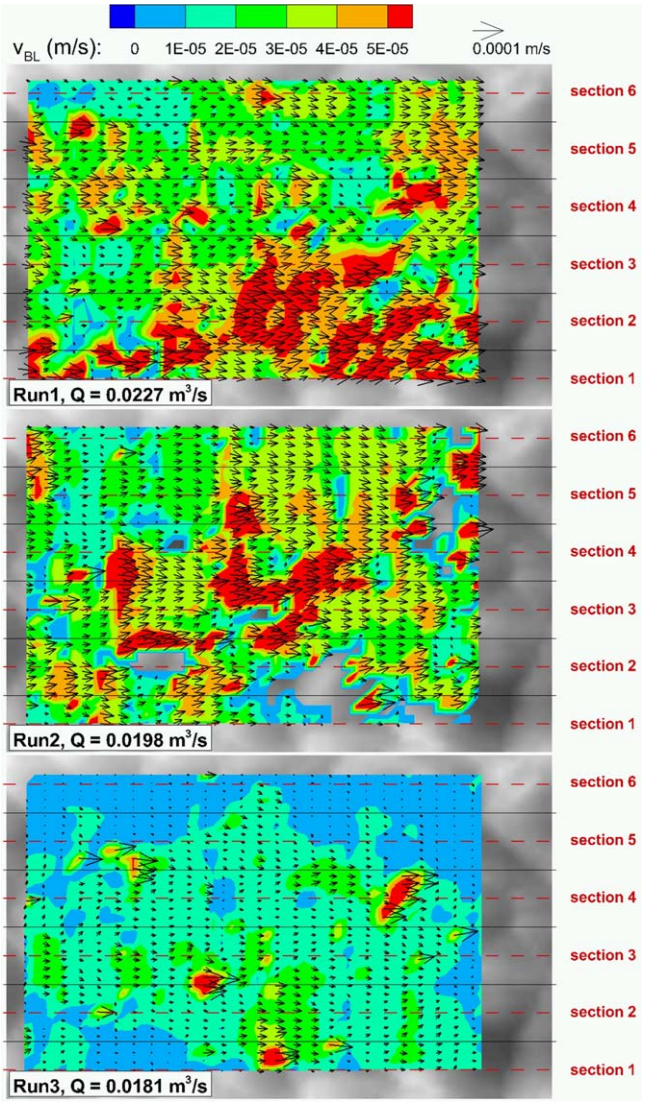

Figure 11. Bed form velocities estimated with image velocimetry software applied to the first image pair of acoustic maps acquired in Run 1, Run 2, and Run 3, respectively. The longitudinal swaths (aligned in the streamwise direction) defined in the figure are used for checking the flow conditions and estimation of the bed load transport rates.

The spatial average values for the first image pairs are $3.50 \cdot 10^{-5}$, $3.11 \cdot 10^{-5}$, and $1.37 \cdot 10^{-5}$ m/s for Run 1, Run 2, and Run 3, respectively. The obtained velocity isocontours reveal variation in the spatial distribution of the vector fields for all the cases. This is attributed to the nonhomogeneous spatial distribution of the bed forms across and along the channel as well as to the flume-induced effects described above. The velocity field for Run 2 shows areas with sparse or no data. Due to the missing vectors the spatially averaged velocity values contain some uncertainty primarily in section 1, which might also increase the uncertainty in the bed load estimation for this run.

The associated assumption employed by most of the previous bed load rate measurement approaches is that the bed form migration is unidirectional. The 2-D velocity maps obtained with AMV represent significant progress compared to previously developed measurement approaches where bed form velocities are estimated only along a line of sight aligned in the streamwise direction. While the assumption is valid for most of the areas illustrated in Figure 11, there are, however, many subareas in each of the AMV maps where the flow is 2-D. This is also expected, as the direction of the flow is dictated by the orientation of the bed forms with respect with dominant flow direction that also show a quasi-2-D distribution in Figure 10. The vector fields plotted in Figure 11 illustrate that the bed form velocities are two-dimensional, revealing a realistic complexity. The applicability of the LSPIV to estimate 2-D velocity fields is important for natural rivers where we expect a considerably larger spatial nonhomogeneity of the bed form orientation and cross-sectional geometry compared with the laboratory conditions.

Section 2.1 of this paper discusses some challenges in acquiring acoustic maps using a scanning protocol. It was mentioned that due to the instrument and measurement protocol limitations, mapping is affected by the movement of the bed. Verification of the impact of the moving bed on the accuracy of the velocity estimations is tested herein by using a customized analysis. The analysis hypothesis is that during the hour-long acoustic mapping, the flow field was quasi-steady and bed forms were in equilibrium. To test this hypothesis, the test section was divided into six longitudinal swaths indicated as sections 1, 2, 3, 4, 5, and 6 in Figure 11. The width of swath 1 and 6, i.e., at the flume sides, was 0.169 and 0.106 m for swath 2, 3, 4, 5. For each swath, the mean velocity values were obtained using only the streamwise component of the velocity across the selected swath. These velocities were used to calculate time-averaged values for the four acoustic image pairs (1-2, 2-3, 3-4, 4-5). The variation of spatiotemporal averages of the velocity distributions

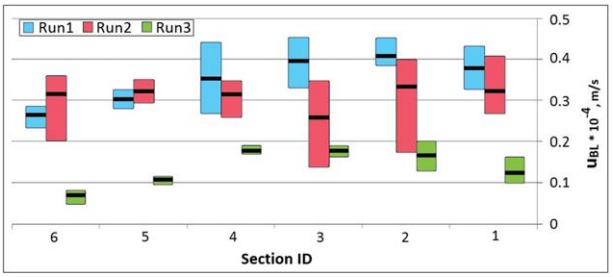

Figure 12. Cross-sectional distribution of mean bed load velocities for the six streamwise swaths forming the cross section in the acoustic maps acquired for Run 1, Run 2, and Run 3. Intervals of variation superposed on the averages for each swath illustrate the max and min values for the velocity used in computing the sample average.

are plotted in Figure 12 for Run 1, Run 2, and Run 3, respectively (swath 1 is located on the right side of the channel). Superposed on the estimated average velocities shown in the figure, are the intervals of variation (max-min) of the average velocities obtained from the four processed image pairs. These intervals capture the temporal variation of the swath averages across the section. These intervals are quite constant (within $\pm$20%) for the swaths covering the cross section in Runs 1 and 3. The intervals are quite different from swath to swath for Run 2 (between $-$45% and 35%). Overall, these post experiment checking tests confirm both the stability of the flow as well as the propriety of the measurement protocols.

A similar spatiotemporal analysis is conducted to assess the bed form homogeneity for each experimental run. While the bed load velocity was analyzed using image pairs, the morphological characteristics of the bed form were obtained from the analysis of individual acoustic images. The characteristic bed form height (Λ) was calculated for each swath, as explained in section 2.3. Using the obtained parameters for each image pair, their spatiotemporal averages were estimated similarly to those of the bed form velocity values. Besides being a geometrical characteristic of the bed form, Λ is also used for estimation of the bed load via the Exner equation. The distribution of Λ for the swaths covering the cross section along with their temporal variability (illustrated with line intervals superposed on the average values) is plotted in Figure 13. The distributions bundled for each section reflects the homogeneity of the bed geometry in the streamwise direction and the stability of the flow during the 1.5 h long experiment for acquiring the acoustic maps.

4.4. Bed Load Rate Estimation

The formula for the estimation of bed load used herein is the Exner equation presented in section 2 of this paper. The equation is applied using bed load velocities obtained with image processing and bed form height using processing tools applied to the acoustic maps. None of the input for the basic bed load rate equation is sampled empirically, rather the needed input is obtained through direct measurements of moving bed forms. The only parameter that is based on prior information is the porosity of the bed material which was assumed $p = 0.4$ as provided by *Gibb et al.* [1984]. With the intention to develop a simple and practical approach, no correction factor was applied for the bed form shape (i.e., the dune shape was assumed to be triangular) in these validation experiments. Alternatively, the bed form shape factor can be calculated using the form factor [e.g., *Ten Brinke et al.*, 1999]. As demonstrated by *Duffy* [2006], the range of the variability of this factor is relatively small. Finally, the last parameter needed in the Exner equation is the density of sediment, evaluated at 2650 kg/m^3 for the present experiments as documented by the provider of the sand material.

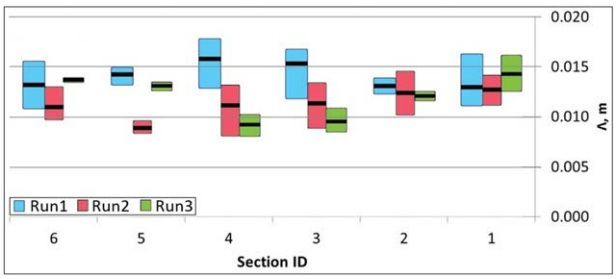

Figure 13. Cross-sectional distribution of the average values of Λ for the six streamwise swaths forming the cross section in the acoustic maps acquired for Run 1, Run 2, and Run 3, respectively. Intervals superposed on the mean values illustrate the max and min values for the velocity used in computing the sample average.

It should be mentioned at this point that, while the bed form geometry and velocities obtained from acoustic and velocity maps are slightly distorted due to the duration of the scanning involved in obtaining individual acoustic maps, the bed load rates are negligibly affected by this distortion. This statement is valid for a fairly uniform and steady flow and bed load rate (as is the case in our experiment) as long as the measurement protocol and its timing are maintained relatively similar. In other words, using the current protocol the bed load rates are obtained using spatiotemporal

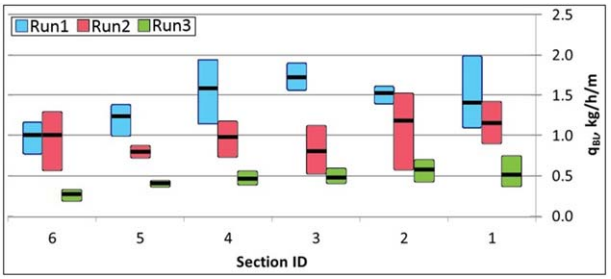

Figure 14. Distribution of bed load transport rates for the six streamwise swaths forming the cross section in the acoustic maps acquired for Run 1, Run 2, and Run 3, respectively.

estimates of the bed form height and velocity acquired via consecutive measurements taken at approximately the same time interval for each of the swaths. This in turn makes the estimation of the bed load independent of the scanning time, while preserving its spatial location as the time between consecutive mappings of the individual swaths is made with a relatively constant time step. From this perspective, it can be stated that the processing protocol used in the current analysis minimizes the effect of distortion involved in scanning the map to almost negligible levels.

Using the same averaging approach for the bed form height and velocity, i.e., averaging the local values along each swath and also in time for the five consecutive measurements, the spatiotemporal bed load rates are determined for the individual swaths oriented in the streamwise direction as shown in Figure 11. The distribution of the time-averaged bed load rates estimated for the individual streamwise swaths for Runs 1, 2, and 3, along with their temporal variability captured by the magnitude of the interval lines superposed on the average values, are plotted in Figure 14. The distribution of the bed load rate estimates across the channel displays slightly larger cross-sectional variability as a result of the combination of individual scattering in the estimation of the bed form velocity and geometry across the flume section. However, it is evident that Run 1 shows the highest rates while Run 3 shows the lowest in each swath. For Runs 1 and 3, it is evident that in the central part of the flume the bed load rates are higher compared with the deeper area along the walls. Run 2 displays a relatively constant distribution. The more dynamic nature of Runs 1 and 2 is reflected by the increased max-min interval of the samples acquired over the time of the experiments. The duration of the experiments was relatively the same. The experimental difficulties encountered with Run 2 are also reflected in the higher scattering of the data sample (however, the variability is less than 50% of the average values). The spatial variability of the bed load rate values, as well as of the other variables related to sediment transport discussed above, emphasize the good performance of the technique that is able to capture details of the flow that are not available from measurements with other bed load instruments.

5. AMV Validation

Using the dynamic and morphologic quantifications enabled by the AMV method, the bulk value of the bed load rate is estimated herein as the weighted average of the cross-sectional values obtained in Figure 14. The weights are commensurate with the swath width. Due to the fact that the MTA scans cannot be acquired close to the flume sidewalls, the weights for the first and sixth swaths are higher. The estimated AMV-based bed load rates per unit width for all the runs of the reported experiments are summarized in Table 3 and plotted in Figure 15. Despite that the flow discharges for the three validation tests were in a narrow range, the bed load transport rates were sensitive to the changes in the flow magnitude and spread over a reasonable distinct bed load range for both the individual swaths (see Figure 14) as well as for the total bed load in the cross section (see Figure 15). This differentiation supports the reliability of the validation tests. The bed load estimates are compared with the direct physical samples acquired with the sand trap in Table 3 and Figure 15. As can be noted from the comparison, the overall agreement between the physical samplings and the AMV based estimations is acceptable. The highest deviation between the direct and indirect methods can be observed for Run 2, where some experimental difficulties occurred in stability of the flow. The instability further affected the instantaneous rates of bed form migration, hence the long-term average (8 h) over which the physical samples were estimated might be different from the 1-h long measurements for constructing the acoustic maps that lead to the AMV bed load rate estimates.

Table 3. AMV-Based Bed Load Rates Estimated for the Experimental Runs Reported in the Study

	Q (10^{-3} m^3/s)	$q_{BL,\ sampled}$ (kg/m/h)	$q_{BL,\ AMV}$ (kg/m/h)
Run 1	22.65	1.37	1.36
Run 2	19.82	0.62	0.99
Run 3	18.12	0.33	0.44

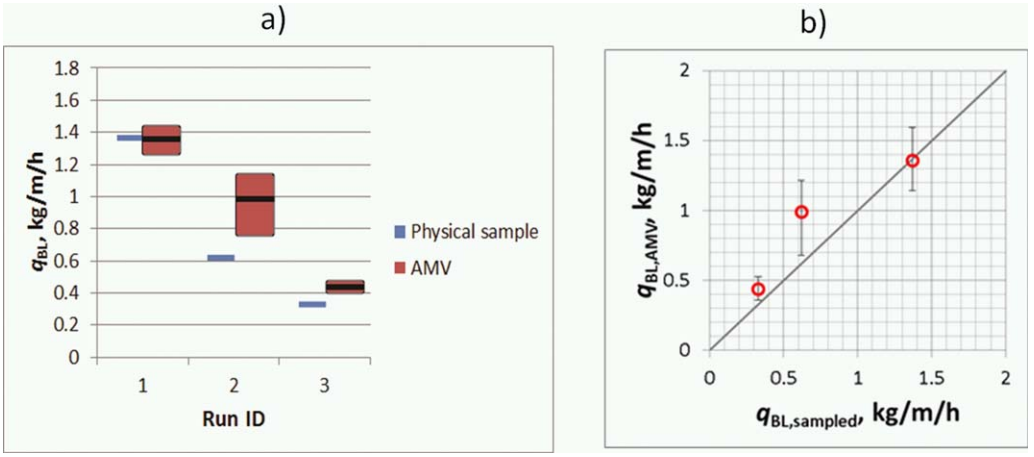

Figure 15. Comparison between bed load rates estimated with AMV and physical sampling: (a) bar plot; (b) agreement plot between AMV and direct physical sampling of the bed load transport rates.

As a consequence, this run resulted in more scattering in all the variables as introduced in the previous section.

6. Discussion

Characterization of the bed form migration is one of the river engineering subjects that still requires significant improvement as it is critical for solving sedimentation problems in alluvial channels. The major obstacle in obtaining a detailed description of the dune-migration morphodynamics is the lack of detailed experimental evidence for closing the gaps in our process understanding and providing benchmark data for validation of the numerous analytical and modeling tools available. The authors of this paper believe that the proposed combination of acoustic and imaging techniques for bed form tracking can significantly contribute to filling in this gap. The nonintrusive nature of the technique and its flexibility in adjusting to the experimental conditions makes AMV a strong candidate for providing transformative insights into bed form migration processes. As a novel technique, however, there are details regarding the assemblage of the instruments and the measurement protocols that have to be further scrutinized and optimized to make the tool widely applicable.

The proof-of-concept experiments for validation of the AMV measurements presented in this paper tackle the observation of the bed form morphodynamics using a mesoscale approach, whereby several dune lengths are ensonified and subsequently analyzed for morphodynamic aspects. The technique can be, however, employed using a macroscale (with acoustic maps covering a swath over the cross-section or even a small river reach) or microscale (within a dune length) approach as subsequently described. While the AMV protocols are similar for various investigative approaches, the instruments are different for laboratory and field conditions commensurate with the range of sounding and their spatiotemporal resolution. Fortunately, there is a wide spectrum of acoustic and optic instruments available to obtain maps in laboratory or field environments. The capability of AMV to "zoom" in to the morphodynamics of the bed form migration modeled in laboratory or occurring in situ is of great interest for both scientific and practical purposes.

AMV is distinct from some of the previous related developmental efforts by its ability to capture 2-D aspects of bed form morphology and dynamics with high spatiotemporal resolution in laboratory and field conditions. The bed load transport rates are determined using a 2-D velocity distribution over the mapped area derived from spatial cross-correlation applied to the actual bed forms produced by the acoustic images. This approach is different from the alternative approaches where the bed form velocity is determined by tracking movement along a preferential direction [e.g., *Lin*, 2011] or by measuring a "virtual velocity" in the proximity of the bed [e.g., *Holmes*, 2010]. Research conducted in the 1960s demonstrated that the rate of sediment transport represented by migrating bed forms gives a more accurate measure of the bed load transport than rates predicted by flow measurements [*Rubin et al.*, 2001].

The AMV protocols can be easily adjusted to provide bed load rate estimates using differences between the volumes of the bed forms at subsequent times [*Abraham and Kuhnle*, 2006]. However, since such a volumetric method is based on subtracting absolute depth values at a point, the results do not capture the information about the dynamics of the bed form migration and can be subject to motion-related artifacts such as long-period heave and tidal errors when it is applied in coastal areas [*Duffy*, 2006]. Moreover, the availability of the velocity distribution associated with individual bed forms can be usefully related to the water velocity in the water column when acoustic mapping is associated with measurements of water velocities over the mapped areas. There are measurement situations when one instrument such as an ADCP provides the information for the acoustic mapping and for velocity in the water column simultaneously [*Holmes et al*., 2010].

While the macroscale AMV implementation approach is similar to the one developed by *Duffy* [2006] for estimation of the bed load transport rates, the same AMV protocols can be used to investigate bed form migration at the meso and microscales. Besides quantification of the bed load transport rates, the mesoscale and microscale AMV approaches enable investigation of the finer aspects of the bed form migration, typically through well-controlled laboratory experiments. Initial efforts were made during these experiments to complement AMV measurements with additional ones acquired with conventional PIV technology to further increase the detail of the investigation (Tsubaki, personal communication). Tackling the AMV with meso or microscale approaches allows for substantiation of bed load transport features such as the formation of the ripples superimposed on bed forms as well as their dynamics, and capturing the movement and clustering of individual sand particles in rolling ripples or as suspended sediment.

Use of AMV for investigation of the finer scale of bed form processes has the potential to shed light on a suite of issues on bed form formation and migration [see e.g., *Gyr and Kinzelbach*, 2004; *Palmer et al*., 2012]. For instance, further research using AMV can clarify questions related to the translation and the deformation of bed forms discussed earlier by *McElroy and Mohrig* [2009]. In their study, the bed form movement was decomposed into two independent constituents, translation and deformation, where the former is the mean downstream migration, whereas the latter is the sum of all changes to the bed's topographic profile measured from within the bed's moving reference frame. They found that bed form deformation can be interpreted as the exchange of sediment between the suspended load and bed load, i.e., represents a vertical flux of bed material which, although insignificant in laboratory experiments, can play an important role in field conditions.

The adoption of the type of AMV approach (i.e., macro, meso, or micro) is dictated by the nature of the study site (laboratory or field) along with the type, configuration, and operational characteristics of the sensor used for mapping. Estimation of the bed load rates with AMV does not require a priori assumptions of bed form spacing and geometry or spatial distribution of their velocity. However, the selection of the scanning time for obtaining an acoustic map and the time between repeated acoustic map acquisitions require knowledge of the flow regime (i.e., steady or unsteady), sediment transport mode, and rough estimates of the bed form migration characteristics. The latter information category includes hydrodynamic and sediment parameters such as flow velocity, bed shear stress, typical grain size, and characteristics of the bed form geometry. With this information, available estimates of the migration rates can be obtained using empirical relationships [e.g., *Lin and Venditti*, 2013].

Similarly, the implementation of the conventional rules of thumb for image velocimetry requires knowledge about the flow velocity and the image patterns that are traced for quantification of the bed form migration dynamics. In the present context, the image patterns can be associated with a variety of visible features in the acoustic maps, from dune crests and elevation gradients to ripples and particle clusters rolling over the dunes. Availability of acoustic maps acquired with high spatiotemporal resolution allows one to use the same raw acoustic maps for macro, meso and, microscale approach. For example, acoustic maps with visible ripples allow for employing the mesoscale approach by zooming in on the analysis area over several dunes. The same maps can be used at their maximum extent to track the movement of the bed form fronts. The zooming process requires commensurate adjustments in the size of the IA and SA windows.

An area of future interest for the AMV implementation is its potential to conduct analysis of bed load transport at the microscale level (i.e., ripples moving atop of bed forms). This kind of utilization of the technique is further pushing the constraints on the spatiotemporal resolution of the imaging and the image-processing methods. High-resolution submersible cameras might be capable of capturing the dynamics of

group of articles within dunes and their interaction. This very fine-scale investigation of sediment movement can answer finer details of the transport process, including aspects related to sheet flows or particle deposition and resuspension in relationship with the transport as captured up to the dune level. As of now, this detailed analysis can only be performed in laboratory environment.

The potential of AMV use in field conditions is of utmost importance for practitioners, as the availability of bulk sediment transport rates across the river cross section is directly linked to several areas of critical socioeconomic importance such as navigation, hydropower capacity, or habitat quality. The bed load transport can be successfully tackled in situ using the AMV macro (river reach) approach with ADCP and MBES measurements. These instruments can rapidly acquire acoustic maps in cross sections as well as along river reaches with minimal effort. It has to be noted, however, that in natural conditions the bed load transport rate represented by bed form movement occurs at the lower limit of the total bed load transport [e.g., *Duffy*, 2006]. Of special importance for the macroscale application of AMV is its capability to map the areas of erosion-deposition, the type of dune regimes developing on streambed in different conditions, and their connection with the flow in the water column and the characteristics of the bed material. Based on the present tests, the authors are confident that AMV is readily applicable in subcritical flow regime for both sand and gravel bed rivers. For particular regimes such as flat bed or antidunes as well as in situations with strong nonuniform bed material, more testing is needed to verify the degree of validity of AMV as presented herein and the formulation of adjustments for adapting the method to these flow cases.

The implementation of the AMV in field conditions follows the same sequencing and rules of thumb for timing of the bed scanning as those described for laboratory conditions. Some of the field instruments for acoustic mapping already have provisions in place that uniquely support AMV implementation. This is the case for MBES; it is well fit both with respect to its native spatiotemporal resolution as well as is in terms of efficiency in data acquisition over large scales. Moreover, the current field measurement practice bundle together in simultaneous measurements form one deployment MBES and ADCP. The ADCP additions empower AMV with readily available information for setting the parameters of the AMV processing. ADCPs are also scrutinized for additional measurement capabilities such as characterization of sheet flows [e.g., *Rennie et al*., 2002, 2007; *Jamieson et al*., 2011] and measurement of the suspended sediment in the water column simultaneously with the acquisition of the 3-D velocity field [e.g., *Kostaschuk et al*., 2005; *Baranya and Józsa*, 2013; *Guerrero et al*., 2014; *Latosinski et al*., 2014]. Collectively, these instruments—as currently deployed for much less ambitious tasks—have the potential to document flow and sediment transport as previously was not conceivable outside of laboratory conditions.

7. Conclusions

The experimental evidence presented in this paper illustrates the capability of AMV to qualitatively and quantitatively assess bed form dynamics and estimate bed load transport rates. The end-to-end measurement protocol described in the paper is generic and can be accomplished using a variety of technological, analytical, and visualization approaches. In essence, it assumes repeated recordings of a sequence of maps of the bathymetry in a moving body of water as a first step. Subsequently, image velocimetry concepts are applied to the acoustic images to infer quantitative information about the bed form migration and potentially other more complex features of the dune movement. The combination of techniques presented here takes advantage of recent advancements in acoustic and image technologies, and it can be asserted that its development stems from their capabilities developed so far for other measurement purposes. The technique can be further improved if bed form dynamics quantification is set as the primary goal in the design of the technique's specifications.

The AMV methodology as presented here is a new and original measurement concept that integrates elements and techniques developed independently over time. AMV is based on emerging acoustic and optical technologies; therefore, it is expected that new developments made in other application areas (i.e., measurement of suspended sediment with hydroacoustics instruments, photogrammetry, scanning technologies, material recognition based on backscatter signal properties) can subsequently improve AMV. The nonintrusive nature and the digital processing and communication technologies available for supporting the acoustic and image-based instruments make it possible to develop AMV operating in real-time. Given the two-dimensional nature of the quantification of the bed form dynamics, the bed load rates can be

estimated along multiple directions (i.e., from streamwise to spanwise) therefore making AMV useful not only in riverine environments but also in coastal applications where the flow can be highly three-dimensional.

This combination of techniques assembled in AMV is fit for implementation in laboratory and field conditions by properly selecting the acoustic sounding sensors. The rules of thumb described for generating the acoustic maps and the considerations on the spatial-temporal features of the data acquisition process, as related to the actual dynamics of the bed forms, are generic and therefore valid for both field and laboratory conditions. AMV is especially well suited and desirable for field data acquired with the increasingly popular acoustic technique for riverine environments, i.e., Acoustic Doppler Current Profilers and Multi-beam Echo-sounders. Targeting in situ measurements with AMV is of special importance not only because it transforms the way the bed load measurements are currently made but because it enables investigation of the bed form migration in a natural environment, circumventing the complex modeling work required to accurately replicate this process in the laboratory conditions.

Acknowledgments
The first and fourth authors were supported by grant 11-TI-C06 of the Ministry of Land, Infrastructure and Transport (Korea). We acknowledge the funding of the second author from the Imre Korányi Scholarship and the János Bolyai fellowship of the Hungarian Academy of Sciences. The first author was partially supported by Project 47/2012 of the "Parteneriate" program, UEFISCDI, Romania. The above mentioned sources of support are gratefully acknowledged. We also thank the associate editor and the three reviewers for their valuable input which led to an improved quality of the paper. The collected and processed laboratory data are available from the corresponding author.

References

Aberle, J., S. E. Coleman, and V. I. Nikora (2012), Bed load transport by bed form migration, *Acta Geophysica*, *60*(6), 1720–1743, doi:10.2478/s11600-012-0076-y.

Abraham, D., and R. Kuhnle (2006), Using high resolution data for measuring bed-load transport, Subcommittee on Sedimentation, 2006, in *Proceedings of the Federal Interagency Sedimentation Conferences, 1947 to 2006,* Reno, Nev. [Available at http://acwi.gov/sos/pubs/ABOUT-CD.pdf.]

Abraham, D., T. C. Pratt, and J. Sharp (2010), Measuring bedload transport on the Missouri River using time sequenced bathymetric data, paper presented at 2nd Joint Federal Interagency Conference, Las Vegas, Nev. [Available at http://acwi.gov/sos/pubs/2ndJFIC/HOME.pdf.]

Abraham, D., R. A. Kuhnle, and A. J. Odgaard (2011), Validation of bed-load transport measurements with time-sequenced bathymetric data, *J. Hydraul. Eng.*, *137*(7), 723–728, doi:10.1061/(ASCE)HY.1943-7900.0000357.

Adrian, R. J. (1991), Particle-imaging techniques for experimental fluid mechanics, *Annu. Rev. Fluid Mech.*, *23*, 261–304, doi:10.1146/annurev.fl.23.010191.001401.

American Society of Mechanical Engineers (ASME) (1989), *Measurement of Fluid Flow in Pipes Using Orifice, Nozzle, and Venturi, ASME MFC-3M-1989*, N. Y.

Baranya, S., and J. Józsa (2013), Estimation of suspended sediment concentrations with ADCP in River Danube, *J. Hydrol. Hydromech.*, *61*(3), 232–240, doi:10.2478/johh-2013-0030.

Cheng, N. S. (2009), Comparison of formulas for drag coefficient and settling velocity of spherical particles, *Powder Technol.*, *189*(3), 395–398, doi:10.1016/j.powtec.2008.07.006.

Chichibu, K., Y. Watanabe, and Y. Shimizu (2008), New imaging technique for measuring fluid and solid velocities in sand-laden flows over dunes in an open channel, paper presented at 5th IAHR Symposium on River, Coastal and Estuarine Morphodynamics, Twente, Netherlands.

Dinehart, R. L. (2002), Bedform movement recorded by sequential single-beam surveys in tidal rivers, *J. Hydrol.*, *258*(1–4), 25–39, doi:10.1016/S0022-1694(01)00558-3.

Duffy, G. P. (2006), Bedform migration and associated sand transport on a banner bank: Application of repetitive multibeam surveying and tidal current measurement to the estimation of sediment transport, Ph.D. thesis, The Univ. of New Brunswick, Fredericton, Canada.

Engel, P., and Y. L. Lau (1981), Bed load discharge coefficient, *J. Hydraul. Div.*, *107*, 1445–1454.

Exner, F. M. (1925), Über die Wechselwirkung zwischen Wasser und Geschiebe in Flüssen, *Sitzungsber. Akad. Wiss. Wien, Math., Naturwiss. Kl., Abt.*, *2A*(134), 165–180.

Fincham, A. M., and G. R. Spedding (1997), Low-cost, high resolution DPIV for measurement in turbulent fluid flows, *Exp. Fluids*, *23*(6), 449–462, doi:10.1007/s003480050135.

Friedrich, H., B. W. Melville, S. E. Coleman, V. Nikora, and T. M. Clunie (2005), Three-dimensional measurement of laboratory submerged bed forms using moving probes, paper presented at 31rd IAHR, Korea Water Resources Association, Seoul, Korea.

Fujita, I., M. Muste, and A. Kruger (1998), Large-scale particle image velocimetry for flow analysis in hydraulic applications, *J. Hydraul. Res.*, *36*(3), 397–414, doi:10.1080/00221689809498626.

Gibb, J. P., M. J. Barcelona, J. D. Ritchey, and M. H. LeFaivre (1984), Effective porosity of geologic materials: First annual report, *SWS Contract Rep. 351*, Ill. State Water Surv., Champaign.

Gray, J. R., J. D. Laronne, and J. D. G. Marr (2010), Bedload-surrogate monitoring technologies, *U.S. Geol. Surv. Sci. Invest. Rep. 2010-5091*, 37 pp.

Guerrero M., N. Ruther, and R. Archetti (2014), Comparison under controlled conditions between multi-frequency ADCPs and LISST-SL for investigating suspended sand in rivers, *Flow Meas. Instrum.*, *37*, 73–82, doi:10.1016/j.flowmeasinst.2014.03.007.

Gyr, A., and W. Kinzelbach (2004), Bed forms in turbulent channel flow, *Appl. Mech. Rev.*, *57*(1), 77–93, doi:10.1115/1.1584063.

Hanes, D. M., V. Alymov, and Y. S. Chang (2001), Wave-formed sand ripples at Duck, North Carolina, *J. Geophys. Res.*, *106*(10), 22,575–22,592 doi:10.1029/2000JC000337.

Helley, E. J., and W. Smith (1971), Development and calibration of a pressure-difference bedload sampler, *U.S. Geol. Surv. Open. File Rep. 73-108*, pp. 1–18.

Henning, M., J. Aberle, and S. Coleman (2010), Analysis of 3D-bed form migration rates, paper presented at International Conference on Fluvial Hydraulics River Flow 2010, Bundesanstalt für Wasserbau, Karlsruhe, Braunschweig, Germany.

Ho, H.-C., M. Muste, S. Plenner, and A. R. Firoozfar (2012), Laboratory considerations for supporting multi-box culvert design, *Can. J. Civ. Eng.*, *40*, 324–333, doi:10.1139/cjce-2012-0201.

Ho, H.-C., M. Muste, and R. Ettema (2013), Sediment self-cleaning multi-box culverts, *J. Hydraul. Res.*, *51*(1), 92–101, doi:10.1080/00221686.2012.757565.

Holmes, R. R., Jr (2010), Measurement of bedload transport in sand-bed rivers: A look at two indirect sampling methods, *U.S. Geol. Surv. Sci. Invest. Rep. 2010-5091*, pp. 239–252.
Jamieson, E. C., C. D. Rennie, R. B. Jacobson, and R. D. Townsend (2011), Evaluation of ADCP bed velocity in a large sand bed river: Moving versus stationary boat conditions, *J. Hydraul. Eng.*, *137*(9), 1064–1071, doi:10.1061/(ASCE)HY.1943-7900.0000373.
Kantoush, S. A., A. J. Schleiss, T. Sumi, and M. Murasaki (2011), LSPIV implementation for environmental flow in various laboratory and field cases, *J. Hydro-environ. Res.*, *5*(4), 263–276, doi:10.1016/j.jher.2011.07.002.
Kostaschuk, R. A., M. A. Church, and J. L. Luternauer (1989), Bedforms, bed material, and bedload transport in a salt-wedge estuary: Fraser River, British Columbia, *Can. J. Earth Sci.*, *26*, 1440–1452.
Kostaschuk, R., J. Best, P. Villard, J. Peakall, and M. Franklin (2005), Measuring flow velocity and sediment transport with an acoustic Doppler current profiler, *Geomorphology*, *68*(1–2), 25–37, doi:10.1016/j.geomorph.2004.07.012.
Latosinski F., R. N. Szupiany, C. M. García, M. Guerrero, and M. Amsler (2014), Estimation of concentration and load of suspended bed sediment in a large river by means of acoustic Doppler technology, *J. Hydraul. Eng.*, *140*(7), doi:10.1061/(ASCE)HY.1943-7900.0000859.
Lin, C.-Y. M. (2011), Bedform migration in rivers, MS thesis, Simon Fraser Univ., Vancouver, B. C., Canada.
Lin, C-Y. M., and J. G. Venditti (2013), An empirical model of subcritical bedform migration, *Sedimentology*, *60*(7), 1786–1799, doi:10.1111/sed.12056.
McElroy, B., and D. Mohrig (2009), Nature of deformation of sandy bed forms, *J. Geophys. Res.*, *117*, F00A04, doi:10.1029/2008JF001220.
Muste, M., and R. Ettema (2000), River-sediment control at Conesville station, on the Muskingum River, Ohio, *IIHR Rep. 410*, Iowa Inst. of Hydraul. Res., The Univ. of Iowa, Iowa City, Iowa.
Muste, M., T. Vermeyen, R. Hotchkiss, and K. Oberg (2007), Acoustic velocimetry for riverine environments, *J. Hydraul. Eng.*, *133*(12), 1297–1299, doi:10.1061/(ASCE)0733-9429(2007)133:12(1297).
Muste, M., I. Fujita, and A. Hauet (2008), Large-Scale Particle Image Velocimetry for measurements in riverine environments. *Water Resour. Res.*, *44*, W00D19, doi:10.1029/2008WR006950.
Muste, M., S. Baranya, R. Tsubaki, D. Kim, H. Ho, D. Tsai, and D. Law (2015), Acoustic Mapping Velocimetry proof-of-concept experiment, paper presented at 36th IAHR World Congress, IAHR, The Hague, Netherlands.
Nordin, C. F. (1971), Statistical properties of dune profiles. Sediment transport in al luvial channels, *U.S. Geol. Surv. Prof. Pap. 562-F*, 40 pp.
Palmer, J. A., R. Mejia-Alvarez, J. Best, and K. T. Christensen (2012), Particle Image Velocimetry measurements of flow over interacting Barchan dunes, *Exp. Fluids*, *52*(3), 809–829, doi:10.1007/s00348-011-1104-4.
Raffel, M., C. E. Willert, and J. Kompenhans (1998), *Particle Image Velocimetry: A Practical Guide*, Springer, N. Y.
Rennie, C. D., R. G. Millar, and M. A. Church (2002), Measurement of bed load velocity using an acoustic Doppler current profiler, *J. Hydraul. Eng.*, *128*(5), 473–483, doi:10.1061/(ASCE)0733-9429(2002)128:5(473).
Rennie, C. D., F. Rainville, and S. Kashyap (2007), Improved estimation of ADCP bedload velocity using a real time Kalman filter, *J. Hydraul. Eng.*, *133*(12), 1337–1344, doi:10.1061/(ASCE)0733-9429(2007)133:12(1337).
Rouse, H. (1939), Experiments on the mechanics of sediment suspension, paper presented at 5th International Congress on Applied Mechanics, Cambridge, Mass., J. Wiley & Sons, London, Chapman & Hall Ltd., N. Y.
Rubin, D. M., G. B. Tate, D. J. Topping, and R. A. Anima (2001), Use of rotating side-scan sonar to measure bedload, paper presented at the Seventh Federal Interagency Sedimentation Conference, Reno, Nev. [Available at https://pubs.usgs.gov/misc/FISC_1947-2006/pdf/1st-7thFISCs-CD/ABOUT-CD.pdf.]
Spasojevic, M., and M. Muste (2002), Numerical model study of Berwick Harbor, Morgan City, Louisiana, *IIHR Distrib. Rep. 422*, IIHR—Hydrosci. and Eng., The Univ. of Iowa, Iowa City, Iowa.
Simons, D. B., E. V. Richardson, and C. F. Nordin (1965), Bedload equation for ripples and dunes, *U.S. Geol. Surv. Prof. Pap. 463-H*, pp. H1–H9.
Ten Brinke, W. B. M., A. W. E. Wilbers, and C. Wesseling (1999), Dune, growth, decay and migration rates during a large-magnitude flood at a sand and mixed sand-gravel bed in the Dutch Rhine river system, *Spec. Publ. Int. Assoc. Sedimentol.*, *28*, 15–32, doi:10.1002/9781444304213.ch2.
Van der Mark, C. F., A. Blom, and S. Hulscher (2008), Quantification of variability in bedform geometry, *J. Geophys. Res.*, *113*, F03020, doi:10.1029/2007JF000940.
Vanoni, V. A. (2006), *Sedimentation Engineering: Theory, Measurements, Modeling, and Practice, Manuals and Reports on Engineering Practice No. 54*, Am. Soc. of Civ. Eng. Publ., Reston, Va.